Chemical Physics 393 (2012) 107–116

Contents lists available at SciVerse ScienceDirect

Chemical Physics

journal homepage: www.elsevier.com/locate/chemphys

VUV photoionization of acetamide studied by electron/ion coincidence spectroscopy in the 8–24 eV photon energy range

Martin Schwell [a,*], Yves Bénilan [a], Nicolas Fray [a], Marie-Claire Gazeau [a], Et. Es-Sebbar [a,1], Gustavo A. Garcia [b], Laurent Nahon [b], Norbert Champion [c], Sydney Leach [c,*]

[a] LISA UMR CNRS 7583, Université Paris Est Créteil and Université Paris Diderot, Institut Pierre Simon Laplace, 61 Avenue du Général de Gaulle, 94010 Créteil, France
[b] Synchrotron SOLEIL, L'Orme des Merisiers, St. Aubin, B.P. 48, 91192 Gif-sur-Yvette Cedex, France
[c] LERMA UMR CNRS 8112, Observatoire de Paris-Meudon, 5 place Jules-Jansen, 92195 Meudon, France

ARTICLE INFO

Article history:
Received 15 October 2011
In final form 24 November 2011
Available online 8 December 2011

Keywords:
Photophysics
Acetamide
Prebiotic photochemistry
Dissociative ionization
VUV
Synchrotron radiation
Interstellar chemistry

ABSTRACT

A VUV photoionization study of acetamide was carried out over the 8–24 eV photon energy range using synchrotron radiation and photoelectron/photoion coincidence (PEPICO) spectroscopy. Threshold photoelectron photoion coincidence (TPEPICO) measurements were also made. Photoion yield curves and branching ratios were measured for the parent ion and six fragment ions. The adiabatic ionization energy of acetamide was determined as I.E. ($1^2A'$) = (9.71 ± 0.02) eV, in agreement with an earlier reported photoionization mass spectrometry (PIMS) value. The adiabatic energy of the first excited state of the ion, $1^2A''$, was determined to be ≈10.1 eV. Assignments of the fragment ions and the pathways of their formation by dissociative photoionization were made. The neutral species lost in the principal dissociative photoionization processes are CH_3, NH_2, NH_3, CO, HCCO and NH_2CO. Heats of formation are derived for all ions detected and are compared with literature values. Some astrophysical implications of these results are discussed.

1. Introduction

Acetamide, $H_3C–C(O)–NH_2$, is one among simple model molecules for the peptide linkage in polypeptides and proteins. Understanding the conformation of these biologically important species can be assisted by knowledge of the structure of this amide. Furthermore, amides are possible precursor molecules in the prebiotic formation of aminoacids that are necessary for the synthesis of proteins [1]. Our previous VUV spectroscopy and photophysics studies on small prebiotic molecules [2], as well as on amino acids [3] and purines and pyrimidines [4], including nucleobases [5], have been carried out in the context of their relevance to exobiological questions. Other groups have been working in this context too [6]. UV and VUV radiation are among the important energy sources impinging on prebiotic and biotic species in astrophysical sites [7].

There have been numerous attempts to prepare these species from simpler compounds under conditions that resemble those of the primitive Earth. For a review on this subject see Ref. [8]. There have also been experimental and theoretical studies of analogous processes in the interstellar medium (ISM) [9,10]. Acetamide has been observed in the ISM by radioastronomy spectral measurements, in both emission and absorption, in the star-forming region Sagittarius B2(N) [11]. The interstellar formation of acetamide is speculated to occur by the exothermic reaction of the methylene radical CH_2 with formamide, the latter being present in this region of space with an abundance five times that of acetamide [11]. Spin is not conserved in this reaction so that an activation barrier could exist. Shocks and UV irradiation could help overcome a barrier to reaction. Models have also been proposed [10] in which acetamide is formed on interstellar grains by radical–radical interactions. The reacting radicals, CH_3 and HNCO, require irradiation of the icy mantles for their eventual formation on the grains. The reaction between these radicals is followed by hydrogenation to form acetamide which is then released to the gas phase, where it is observed by radioastronomy, by warm-up mechanisms. Fair agreement with the observed abundance of acetamide in the ISM has been obtained with at least one theoretical model [10].

We remark also that acetamide has been synthesized in laboratory studies involving UV photolysis and proton irradiation of interstellar and pre-cometary ice analogues, such as frozen

* Corresponding authors. Tel.: +33 1 4517 1521; fax: +33 1 4517 1564 (M. Schwell), tel.: +33 1 4507 7561; fax: +33 1 4507 7100 (S. Leach).
E-mail addresses: Martin.Schwell@lisa.u-pec.fr (M. Schwell), Sydney.Leach@obspm.fr (S. Leach).
[1] Present address: King Abdullah University of Science and Technology, Saudi Arabia.

0301-0104/$ - see front matter © 2011 Elsevier B.V. All rights reserved.
doi:10.1016/j.chemphys.2011.11.032

mixtures of H_2O, CH_3OH, NH_3 and CO [12]. However, acetamide has not yet been observed in comets.

In this work we have carried out a VUV photoionization study using synchrotron radiation and electron/ion coincidence spectroscopy in the 8–24 eV energy range. The results are important for the determination of survival conditions of this prebiotic molecule to VUV radiation in an astrophysical context. In addition, the study and interpretation of the products of dissociative photoionization of acetamide have potential repercussions, in particular, relative to the use of mass spectrometry in peptide sequencing, which requires an understanding of the chemistry of amides in the mass spectrometer. Earlier photoionization mass spectrometry (PIMS) studies on acetamide have been carried out by Watanabe et al. [13], who measured the ionization energy, and by Schröder et al. [14] who studied keto/enol isomerization of the acetamide cation. In the latter study, quadrupole mass spectrometry has been used and appearance energies (AE) were reported too, but no ion yield curves or branching ratios.

2. Structural aspects

2.1. The structure of neutral acetamide

The acetamide molecule is considered to be planar and to have C_s symmetry [15,16]. Electron diffraction data [17] are compatible with a planar structure, but neutron diffraction studies [18] have shown that the peptide moiety in acetamide is slightly non-planar. In the present study we consider acetamide as effectively planar, as is compatible with infrared spectroscopy studies in the gas phase [19,20].

Ab initio molecular orbital studies on the structure of acetamide [21] show that the most stable conformation is that in which the methyl group is staggered with respect to the N–C bond. The methyl group is thus eclipsed with respect to the C=O link. The barrier to rotation of the methyl group with respect to the N–C bond is ≈740 meV, determined by NMR for acetamide in solution [22]. Calculated values are 635–890 meV, according to the level of calculation [21], and 542 meV, in *ab initio* calculations which include polarization functions in the basis set [23]. We note that, like formamide, acetamide can be considered to have two resonant structures, which give the C–N bond partial double bond character with a planarised nitrogen atom.

2.2. Electronic structure

According to Asbrink et al. [24] the electron configuration of the planar C_s acetamide molecule is:

$$\ldots(5a')^2(6a')^2(7a')^2(8a')^2(9a')^2(1a'')^2(10a')^2(11a')^2 \times (12a')^2(2a'')^2(3a'')^2(13a')^2$$

The a′ M.O.s are σ orbitals, the a″ are π orbitals. The two highest occupied orbitals are close together. All interpretations of the photoelectron spectra (PES) of acetamide [24–29] respect the above order of the two highest M.O.s.

3. Experimental

Measurements were performed at the undulator beamline DESIRS [30] of the Synchrotron Soleil (St. Aubin, France). The permanent endstation named SAPHIRS, on one of the two monochromatised branches of this beamline, was employed for our measurements. The beamline incorporates a 6.65 m normal incidence monochromator [31] which is equipped with four different gratings. For our measurements, we used the 200 grooves/mm grating which provides a constant linear dispersion of 7.2 Å/mm at the exit slit of the monochromator. The typical slit width used in our experiments is 100 μm, yielding a monochromator resolution of 0.7 Å for these conditions (about 6 meV at $h\nu$ = 10 eV and 18 meV at $h\nu$ = 18 eV). We also note that the beamline is equipped with a gas filter [32], which effectively removes all the high harmonics generated by the undulator that could be later transmitted by the grating, providing a high spectral purity. In this work, Ar has been used as a filter gas for all measurements below 16 eV.

The DELICIOUS II apparatus has been described in detail recently [33]. Briefly, it consists of a photoelectron photoion coincidence (PEPICO) spectrometer combining velocity map imaging (VMI) of the photoelectrons with a linear time-of-flight mass analyzer operating according to Wiley–MacLaren space focusing conditions. From the electron images, zero kinetic energy electrons can be selected in order to measure Threshold-PEPICO (TPEPICO) mass spectra with resolutions as small as 1 meV. In TPEPICO energy scans, the total resolution is given by the convolution of the monochromator's resolution and the energy resolution of the threshold electrons. The latter can be chosen *a posteriori* by changing the size of the central area of the VMI image used for the coincidence measurement within an interval depending on the selected extraction field (cf. [33] for more details). In PEPICO energy scans, giving partial ion yields, electrons with a maximum kinetic energy (KE_{max}) of up to 0.95 eV are used for the coincidence measurements in this study, i.e. there is no ion discrimination up to 0.95 eV above the onsets. KE_{max} depends on the extraction field applied in DELICIOUS II (95 V/cm in our case; cf. Ref. [33]). The spectral resolution of these scans is defined only by the slit widths of the monochromator (see above). The step size in the ion yield curves is 5 meV. The energy scale was calibrated using known absorbing Ar lines from the gas filter. The absolute energy precision is better than 3 meV. All photoion yield curves were normalized with respect to the incoming photon flux, continuously measured by a photodiode (AXUV100, IRD).

Due to its low vapour pressure, the solid acetamide powder (from Sigma Aldrich, no further purification) was placed inside an in-vacuum oven heated to 80 °C. The resulting vapour was mixed with 1 bar of He and expanded through a 50 μm nozzle. The molecular beam then traversed a 1 mm skimmer to enter the ionization chamber, where it intersected the VUV photon beam whose transverse dimensions are about 200 μm (horizontal) × 100 μm (vertical).

We remark that our PEPICO fragment ion appearance energies (AEs) correspond to *effective* thermochemical energy values. The two main factors for the possible difference between the measured AE and the 0 K value are (a) the limited detection sensitivity and (b) the thermal energy stored in the parent neutral. Fragmentation dynamics (possible activation barriers, formation of vibrationally excited fragments) also influence the effective AE. This has been discussed in more detail earlier [34]. In the present molecular beam experiment, the expected low temperature (∼40 K) should, however, provide a value closer to the AE_{0K} than room temperature experiments. Also, compensatory effects may lead to appearance energies that reflect reasonably well their 0 K values as has been pointed out by Chupka [35].

The AEs are determined from semi-log ion yield plots in the threshold region by fitting straight lines to the noise and to the ion signal rise in this region (not shown in our figures). The photon energy at the intersection of these two lines is assigned to the measured AE value. Applying different fits, the precision is estimated by visual inspection of the variation of the intersection and is thus a function of the sharpness of the ion signal rise in the threshold region. Ion yield curves are shown on a linear scale in the figures in order not to distort the shape of the spectrum. The yields for

the various ions are given as a percentage of total yield in these figures, and as normalized intensity for the *m/z* 15 ion (Fig. 6) as discussed in Section 4.3.8.

The measured AE's are used to calculate enthalpies of formation of fragment ions m_1^+ for different possible fragmentation pathways, using Eq. (2):

$$M + h\nu \rightarrow M^+ + e^- \rightarrow m_1^+ + m_i + e^- \quad (1)$$

$$AE + \Delta_f H_{gas}(M) - \Sigma[\Delta_f H_{gas}(m_i)] = \Delta_f H_{gas}(m_1^+) \quad (2)$$

The $\Delta_f H(m_1^+)$ values determined from Eq. (2) are then compared to tabulated standard thermochemical enthalpies of formation, thus permitting assignment of particular fragmentation channels. If literature $\Delta_f H(m_1^+)$ values are not available, our values represent new, upper limit values of these entities.

In Table 1 we report the *m/z* peaks observed at 21 eV photon excitation energy and the corresponding appearance energies. The ionic and neutral products of the dissociative ionization processes given in this table result from the discussion in Section 4.3.

4. Results and discussion

4.1. The photoion mass spectrum

The mass spectra were recorded at a series of photon excitation energies between 10.5 and 13 eV and between 18 and 24 eV. The TOF mass spectrometer has about 100% transmission efficiency, independent of mass, so that the observed relative intensities reflect true branching ratios at each excitation energy. In our experiment, the ions have about 3.5 keV kinetic energy when impinging on the detector so that the mass dependence of the MCP sensitivity can be neglected (cf. [36]). Low photon energy excitation mass spectra are presented for E_{exc} = 10.5 eV (Fig. 1a) and 12 eV (Fig. 1b). At 10.5 eV only the parent ion at *m/z* 59 as well as its ^{13}C isotopic sibling at *m/z* 60. The *m/z* 60 mass peak probably contains a contribution of protonated acetamide since its intensity is higher than the 2.6% expected for the ^{13}C isotopomer (the *m/z* 17 ion present in this mass spectrum is due to an ammonia impurity arising from thermal dissociation of acetamide, see later). At E_{exc} = 12 eV several fragment ions appear, in addition to the parent ion: *m/z* 44, 43, 42, 31, and 18. At 14.6 eV, CH_3^+ (*m/z* 15) also appears (cf. Table 1). We remark that in our photoion mass spectra each peak exhibits a tail towards longer times-of-flight. This is due to the effects of an inhomogeneous electric field under VMI extraction conditions [33].

At higher excitation energies a series of mass spectra has been recorded up to 24 eV, but no ion yield scans. We show examples

Table 1
Acetamide Photoion Mass Spectrum at E_{exc} = 21 eV: Ion and neutral product assignments and appearance energies.

m/z	Ion	Neutral product	Ion appearance energy (eV)
59	$H_2NC=OCH_3^+$	–	9.71 ± 0.02
44	$NH_2–C=O^+$	CH_3	10.88 ± 0.03 (11.6 EI, [48])
43	$CH_3\ CO^+$	NH_2	11.19 ± 0.05 (11.7 EI, [48])
42	$CH_2=C=O^+$	NH_3	11.25 ± 0.05
41	$C_2H_3N^+$	H_2O	
	$HCCO^+$	NH_3 + H	
31	$CH_2NH_3^+$	CO	10.71 ± 0.03
18	NH_4^+	HCCO	10.77 ± 0.03
17	NH_3^+ impurity		10.16 ± 0.03
	NH_3^+	CH_2CO	
15	CH_3^+	H_2NCO	14.60 ± 0.05
14	CH_2^+	H_2NCHO	n.d.

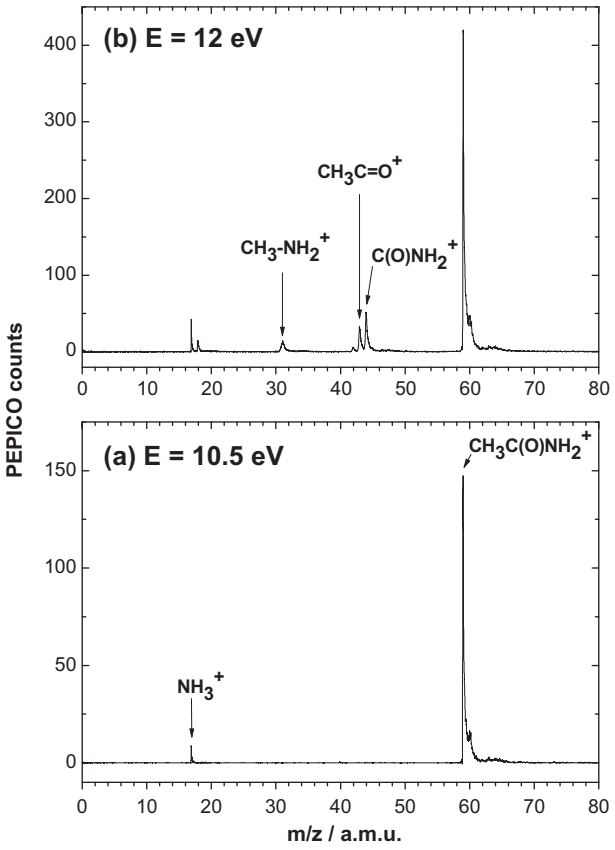

Fig. 1. Photoionization mass spectra of acetamide. (a) 10.5 eV and (b) 12 eV photon excitation energy (PEPICO).

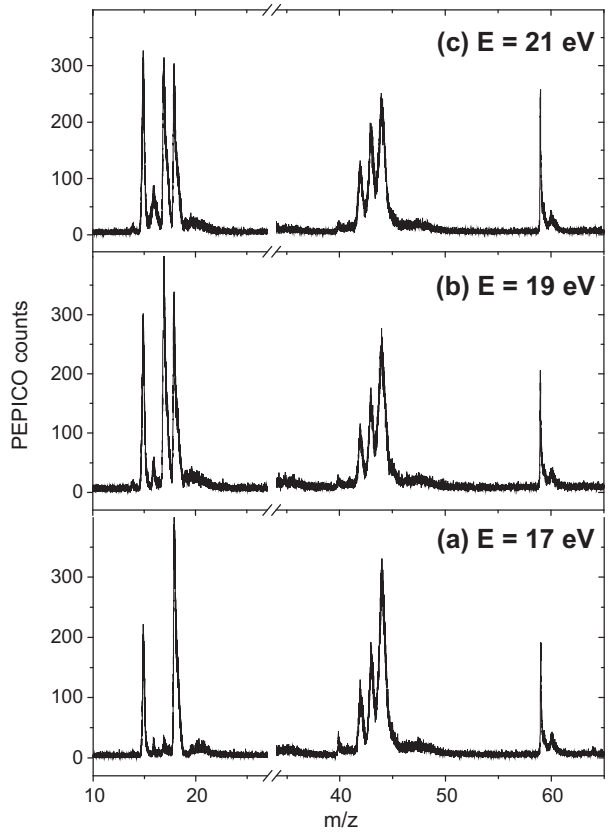

Fig. 2. Photoionization mass spectra of acetamide. (a) 17 eV, (b) 19 eV and (c) 21 eV photon excitation energy (PEPICO).

at E_{exc} = 17, 19, and 21 eV in Fig. 2. They resemble grossly to the 70 eV electron impact mass spectra (EI-MS) [37,38] whose principal mass peaks are *m/z* 59, 44, 43, 42, 41, 28, and 15. In both EI studies, the parent ion is the base peak of the mass spectrum. This is in contrast to our photon impact mass spectrum as can be seen in Fig. 2, most probably because KE_{max} of the photoelectrons is limited to 0.95 eV in our study. The intensity ratios of the principal fragment ions, however, vary only slightly in the three studies [37,38], and ours. Besides mass discrimination effects due to different experimental methodologies, slight differences may be due to differences between photon impact and electron impact excitation processes, as discussed elsewhere [39].

The fragment *m/z* 28 is not seen in our study below the N_2 ionization threshold (15.581 eV). In the case of EI studies, it might therefore be due to residual N_2, which is always difficult to exclude. The NIST EI-MS [37] also reports relatively strong ions of *m/z* 18 and 17 but Gilpin [38] does not. We see these ions at higher energies too, however in this energy regime they are partly due to the water contamination of the hygroscopic sample.

Weak ions (<5% rel. int.), with *m/z* 45, 40, 39, 38, 31, 30, 29, 27, 16, and 14 are also observed in the EI studies. Most of them do not appear in our photon impact mass spectra up to an excitation energy of 24 eV, except for *m/z* 31 below 15 eV (cf. Fig. 1), *m/z* 16 and 14. *m/z* 40 in our mass spectra in Fig. 2 is due to an Ar^+ impurity. *m/z* 16 is first observed in very low intensity in a mass spectrum taken at *E* = 15.5 eV (not shown). With appearance energy data found in the NIST database [37], it can be concluded that this mass peak is most probably due to NH_2^+ formed by dissociative ionization of NH_3 which is present in our heated sample. The peak at *m/z* 14 is first observed in very low intensity at E_{exc} = 17 eV (cf. Fig. 2a). It is tentatively assigned to CH_2^+ (see discussion in Section 4.3.9).

4.2. The parent ion m/z 59

4.2.1. Ionization energies

Fig. 3a shows the TPEPICO yield curve of the parent ion, *m/z* 59 recorded with a resolution of 10 meV. It provides measurements of the vertical and adiabatic ionization energies of acetamide. The maximum of the first sharp band is attributed to vertical IE so that IE_{vert} = (9.74 ± 0.02) eV. The beginning of the first sharp rise is attributed to the adiabatic IE so that IE_{ad} = (9.71 ± 0.02) eV (see Fig. 3). The weak band seen at 9.69 eV is most probably a hot band. For the sake of completeness, we also show the *m/z* 59 PEPICO spectrum (Fig. 3b). The spectral resolution here is 6 meV. Note that the IE_{ad} read from the PEPICO spectrum is also 9.71 eV (neglecting a small hot band contribution).

IE_{vert} and IE_{ad} values will be discussed below and compared with literature values, but first we discuss the structure of the cation in its ground and first excited electronic states.

There have been relatively few studies of the structure of the acetamide cation. Four possible tautomers have been considered in Refs. [40,41]: They are shown in Scheme 1.

Mourges et al. [40] and Drewello et al. [41] have explored, both experimentally and theoretically, aspects of the potential energy surface of $C_2H_5NO^+$ isomers. The neutral keto form of acetamide is thermochemically more stable than the enol form, with a high energy barrier of the order of 2 eV between them [14]. The cation of the enol (tautomer II), however, is calculated to be 710 meV [41] or 820 meV [40] lower in energy than ionized acetamide in its keto form I. The tautomers III and IV are calculated by Mourges et al. [40] to be, respectively, 190 meV *below* and 473 meV *above* species I (see Scheme 1b).

One might expect negligible isomerisation between ionized acetamide I and its enol tautomer $CH_2{=}C{-}(OH)NH_2^+$ (II) since the latter is separated from the acetamide ion by a substantial barrier, calculated to be 1.52 eV [41] or 1.16 eV [40]. However, experiments in which the products of photoionization are monitored chemically, after a delay in the microsecond regime [14], have shown that keto-enol isomerisation of the acetamide ion occurs at an excitation energy of 10.42 eV, the threshold energy for an enol specific product. This implies that the effective barrier height for keto-enol isomerisation of the acetamide ion is only about 740 meV.

In Table 2 we compare our IE values for acetamide with values obtained from the PIMS measurements of Watanabe et al. [13] and of Schröder et al. [14], as well as with values reported in photoelectron spectroscopy studies. Our adiabatic energy value is 60 meV smaller than that of Watanabe et al. [13] but agrees well with that of Schröder et al. [14] considering experimental errors. It is greater than the PES value of McGlynn et al. [28,29]. However, the latter value is given without error bars and must have a subjective evaluation, as judged from the acetamide photoelectron spectrum given in Fig. 2 of Ref. [28]. Our vertical IE is 120–260 meV smaller than those obtained by HeI photoelectron spectroscopy.

In Table 2 we have also compared the vertical values of ionization of the second highest occupied orbital, a π M.O. On the basis of the difference between vertical IE's given in this table, the experimental energy separation between the excited $1^2A''$ π state and the ground $1^2A'$ σ state is about 400 meV. OVGF calculations give 50 meV [27] while HAM/3 calculations give ⩾400 meV [24]. The corresponding experimental value for the analogous states in formamide is 330 meV [39]. The adiabatic ionization energy of the π orbital in acetamide can therefore be estimated as approximately 9.7 + 0.4 eV ≈ 10.1 eV, assuming the geometry of the $1^2A'$

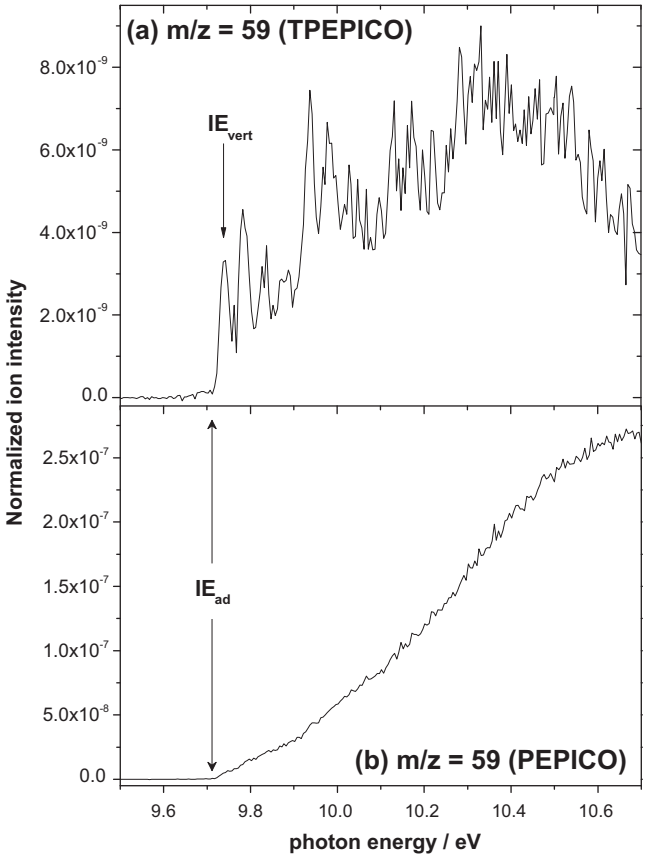

Fig. 3. (a) TPEPICO (resolution ~10 meV) and (b) PEPICO (resolution ~6 meV) spectra of the acetamide parent ion (*m/z* 59) between 9.5 and 10.7 eV photon excitation energy. Vertical and adiabatic ionization energies are indicated by arrows.

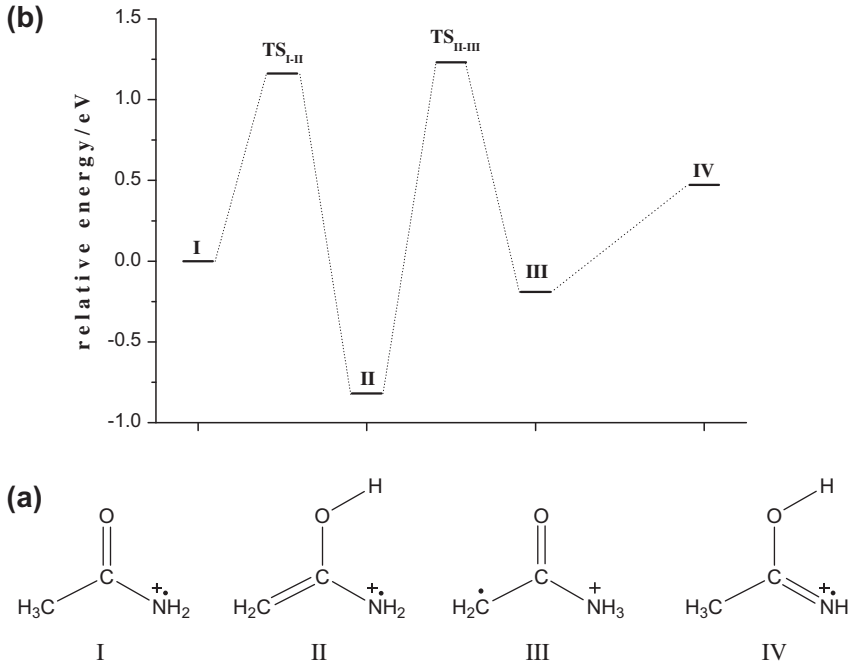

Scheme 1. (a) Four possible tautomers of the acetamide cation and (b) their energies and barriers of conversion according to Ref. [40].

and $1^2A''$ electronic states of the ion to be similar. In the TPEPICO spectrum, which exhibits considerable vibronic structure (Fig. 3a), and whose detailed analysis is ongoing, there is a notable band at ≈10.10 eV which we tentatively assign to the origin band of the excited $1^2A''$ π state of the ion.

The acetamide ion can therefore nominally exist as a σ ($^2A'$) or a π ($^2A''$) radical (cf. Table 2) and the chemistry of such radicals is expected to be different [39]. However, this difference would only be clearly demonstrated if the σ ($^2A'$) or a π ($^2A''$) states can act as isolated states. Whether this is the case merits discussion: If there is no σ–π interaction, a σ radical cation would then be generated at 9.71 eV and a π radical cation at about 10.1 eV. In the σ system, the charge is localized on the carbonyl carbon atom [41], whereas in the π system the charge is distributed over the O, C, and N atoms. However, the close proximity of these two electronic states favours their interaction so that the fragmentation of the ion at higher energies would be not from isolated states but from the ground state, of mixed σ and π parentage, as conjectured by the quasi-equilibrium theory of mass spectra [42]. Dissociation channels, which become active above 10.71 eV (CO-loss channel, Table 1), will explore the vibronic configurational space that has mixed percentage parentage of the σ and π states. We note, however, that for a molecule as small as acetamide, the possibility can exist of well-separated higher electronic excited states acting as isolated states. In that case, dissociation processes localized to these states can occur, and even fluorescence could be observed from such excited states, if the competitive time-scales are favourable [43]. In this respect it is of interest that there is a $2^2A''$ electronic state of the acetamide ion at 13.0 eV [24]. The ≈3 eV energy gap between the $2^2A''$ and the $1^2A''$ ion states could possibly satisfy isolated states criteria [43]. We note that the threshold energy of 10.42 eV for keto-enol isomerisation of the acetamide ion [14] is below that of the lowest dissociation channel which is at 10.71 eV (Table 1). Thus the configurational space explored must include this isomerisation above 10.42 eV; its relative importance is unknown as yet.

4.2.2. Heat of formation of the acetamide parent cation

The heat of formation of acetamide is reported as $\Delta_f H$ (H_2NCHO) = (−2.469 ± 0.008) eV [44]. Using our value IE_{ad} = (9.71 ± 0.02) eV, the heat of formation of the acetamide cation becomes (7.24 ± 0.02) eV. The listed value in the compilation of Lias et al. [44] is given as 7.18 eV, based on a value of IE_{ad} = 9.65 ± 0.03 eV derived from an early measurement by Vilesov [45].

4.3. Fragment ions

Compared to the parent ion, the fragment ions of acetamide formed by dissociative ionization are quite weak in the energy range where they appear (cf. Fig. 1b). Also, the oven temperature could not be raised further in order to increase the signals because

Table 2
Adiabatic and vertical ionization energies of acetamide.

σ IE_{ad} (eV)	σ IE_{vert} (eV)	π IE_{vert} (eV)	ΔIE_σ (meV)[a]	ΔIE_π (meV)[b]	Technique	Reference
9.71 ± 0.02	9.74 ± 0.02		30		TPEPICO-MS	Present study
9.68 ± 0.03					PIMS	[14]
9.77 ± 0.02					PIMS	[13]
9.80	9.96	10.32	160	360	PES	[26]
9.62	9.95	10.34	330	390	PES	[28,29]
(9.62)	10.0	10.4		400	PES	[24]
	9.86	10.32		460	PES	[27]

[a] $\Delta IE_\sigma = (\sigma\ IE_{vert} - \sigma\ IE_{ad})$.
[b] $\Delta IE_\pi = (\pi\ IE_{vert} - \pi\ IE_{ad})$.

already at 80° C, some decomposition is observed (see discussion on *m/z* 17). This is the reason why their AEs are determined from PEPICO curves only. The TPEPICO signal with appropriate resolution is too weak in order to realize a threshold evaluation.

In this section we assign the fragment ions whose AEs were measured (*m/z* 44, 43, 42, 18, 17, 15; see Figs. 4–6) and discuss the corresponding dissociative ionization processes. The other ions observed in the photoion mass spectra (Table 1) are too weak for their yield curves to be measured but the assignments of some are discussed. The breakdown diagram for the measured ions yields is presented in Section 4.4.

4.3.1. m/z 44

The *m/z* 44 ion yield curve, given in Fig. 4a, corresponds to the CH_3 loss channel. The fragment cation has the elemental composition $[N,H_2,C,O]^+$. There are several possible structures for this ion [46] but the most probable form is $H_2N–CO^+$, formed by rupture of the C–C bond in the parent ion. That this ion is indeed H_2NCO^+ is confirmed by the CID mass spectrum of acetamide [47].

The appearance energy of the H_2NCO^+ ion is AE = (10.88 ± 0.03) eV. Thus the C–C bond dissociation energy in the acetamide cation is only (1170 ± 50) meV. A slightly higher PIMS AE value, (11.00 ± 0.04) eV, was observed in Ref. [14]. The reported electron impact AE for *m/z* 44 is 11.6 eV [44] which is much higher than our photon impact value, and this to a surprising extent, considering that the photoion yield curve of Fig. 4a shows a considerable signal at 11.6 eV.

From our AE we calculate $\Delta_fH(H_2NCO^+)$ = (6.90 ± 0.04) eV. This is smaller than the 7.26 eV value given in the Lias et al. compilation [44] but agrees well with the value $\Delta_fH(H_2NCO^+)$ = 6.96 eV that Hop et al. [47] found experimentally from the *m/z* 44 AEs observed in an EI mass spectral study of four different precursor molecules

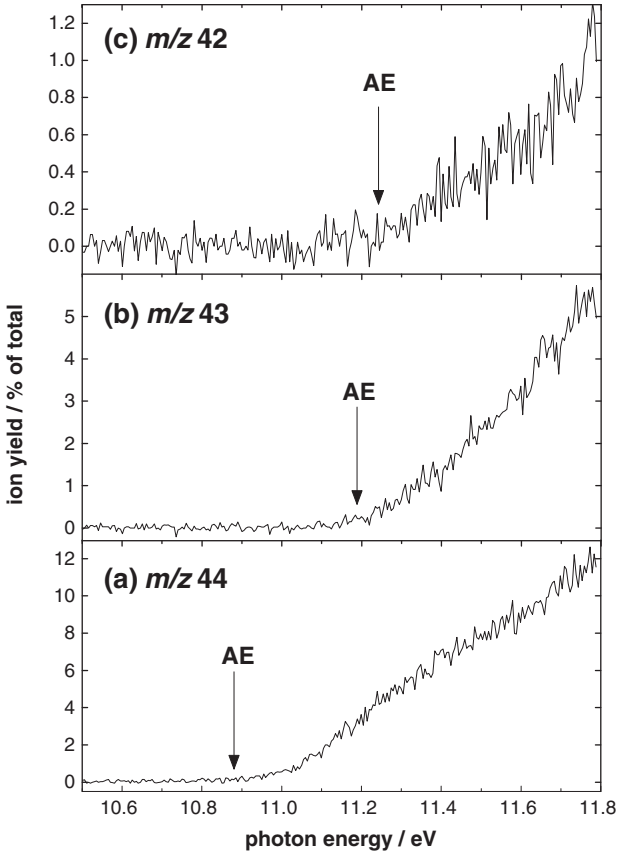

Fig. 4. Photoion yield curves (PEPICO) of acetamide fragment ions. (a) *m/z* = 44. (b) *m/z* = 43. (c) *m/z* = 42. Arrows indicate the respective appearance energies (AEs).

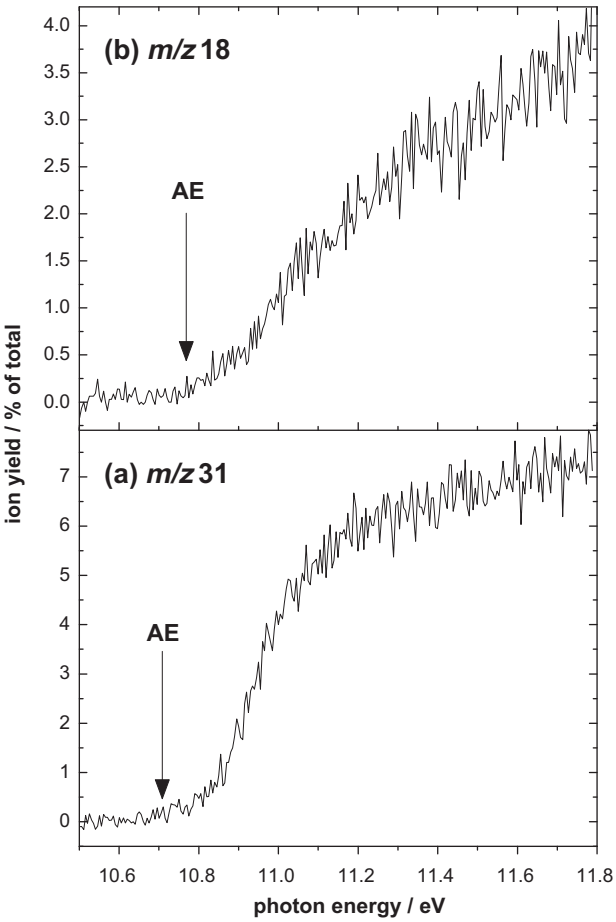

Fig. 5. Photoion yield curves (PEPICO) of acetamide fragment ions. (a) *m/z* = 31. (b) *m/z* = 18. Arrows indicate the respective appearance energies (AEs).

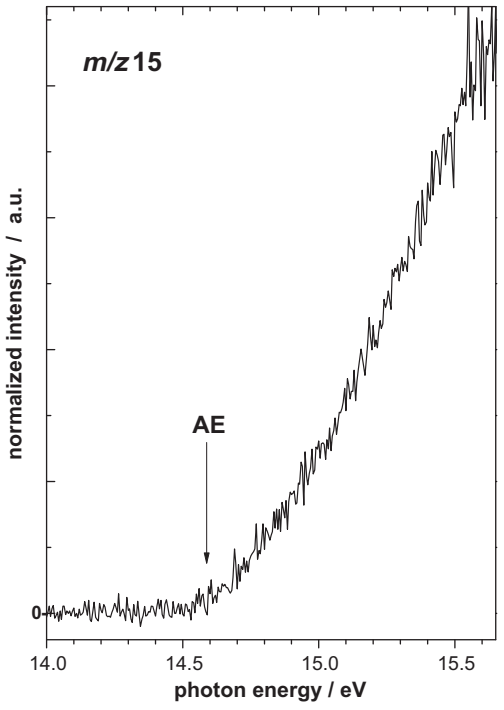

Fig. 6. Photoion yield curve (PEPICO) of acetamide fragment ions. *m/z* = 15. The arrow indicates the appearance energy (AE).

(including acetamide). Hop et al. [47] also derived a value from the proton affinity of isocyanic acid, HNCO, yielding $\Delta_f H(H_2NCO^+)$ = 7.04 eV. However, no error bars are given in this work so it is difficult to relate their EI values to our PI data.

We note also that our heat of formation is slightly smaller but is in satisfactory agreement with $\Delta_f H(H_2NCO^+)$ = (7.10 ± 0.01) eV obtained, in a recent PIMS study of formamide, from the AE of the H-loss reaction in this cation [39].

4.3.2. m/z 43

This ion is assigned to the acetyl cation, CH_3CO^+, that is formed by loss of NH_2. Its ion yield curve (Fig. 4b) provides the appearance energy AE = (11.19 ± 0.03) eV, in good agreement with a previous PIMS value AE = (11.24 ± 0.06) eV [14]. An electron impact value of AE = 11.7 eV has been reported in Ref. [48].

From our appearance energy, and using $\Delta_f H(NH_2)$ = −1.973 eV [37], we determine the heat of formation of this fragment ion to be $\Delta_f H(CH_3CO^+)$ = (6.748 ± 0.058) eV. Our value of the heat of formation of the acetyl ion is (85 ± 69) meV below the value $\Delta_f H(CH_3CO^+)$ = (6.833 ± 0.011) eV listed by Holmes et al. [46]. A value of $\Delta_f H(CH_3CO^+)$ = 6.632 eV has also been reported [49]. We note that the acetyl cation is by far the lowest energy isomer of the nine $[C_2H_3O]^+$ ions studied theoretically by Nobes et al. [49] so that our appearance energy validates assigning *m/z* 43 to this ion. The reaction is an α-cleavage which yields $CH_3CO^+ + NH_2$, in competition with the $H_2NCO^+ + CH_3$ channel discussed above. This dissociation could take place from one or both of the keto (I) and enol (II) ion structures. The intensity ratio of the H_2NCO^+ to the CH_3CO^+ ion in the 70 eV EI mass spectra is of the order of 1.4 [37,38] and there is a similar intensity ratio in our photon impact mass spectra at excitation energies $E_{exc} \geqslant 12$ eV, which indicates that the $H_2NCO^+ + CH_3$ reaction channel is favoured over this excitation energy range.

An alternative assignment of *m/z* 43 is to the $HNCO^+$ ion, which can be formed by CH_4-loss via an ion-neutral complex. A high resolution mass spectrometric study of acetamide has shown that this channel is responsible for only 9% of the *m/z* 43 ions formed by 70 eV electron impact on acetamide [50]. The calculated AE($HNCO^+$) = 12.236 eV, is over 1 eV above the observed AE (*m/z* 43), so that at threshold for the appearance of *m/z* 43 the ions are exclusively CH_3CO^+.

4.3.3. m/z 42

This is assigned to the ketene cation $CH_2{=}C{=}O^+$, formed by NH_3 loss. The appearance energy, AE = (11.25 ± 0.05) eV (Fig. 4c) is in satisfactory agreement with the PIMS AE = (11.13 ± 0.07) eV of Schröder et al. [14]. It is considerably smaller than AE = 11.7 eV reported in an electron impact study [48], which is understandable, given the very slow rise of the *m/z* 42 ion in the threshold region (cf. Figs. 4c and 7). Our fragment ion assignment is confirmed by the heat of formation of the *m/z* 42 ion, $\Delta_f H$ ($CH_2{=}C{=}O^+$) = (9.257 ± 0.062) eV, that we determine from our AE using $\Delta_f H(NH_3)$ = (−0.476 ± 0.04) eV [44]. The NIST compilation gives $\Delta_f H(CH_2{=}C{=}O^+)$ = 9.108 eV [37], based on a value $\Delta_f H(CH_2{=}C{=}O)$ = −0.539 eV [51] for the heat of formation of neutral ketene. Our value $\Delta_f H(CH_2{=}C{=}O^+)$ = (9.257 ± 0.062) eV is closer to that, $\Delta_f H(CH_2{=}C{=}O^+)$ = (9.119 ± 0.030) eV, obtained using the earlier accepted value $\Delta_f H(CH_2{=}C{=}O)$ = −0.494 ± 0.026 eV [52].

The (150 ± 60) meV excess energy in our experimental value of $\Delta_f H(CH_2{=}C{=}O^+)$, as compared with that in the NIST compilation, probably reflects the existence of a complex pathway in creating the ketene cation from acetamide. A possible pathway involves prior isomerisation to an intermediate ion $H_3N\cdots CH_2{=}C{=}O^+$, existing at a potential energy minimum at a 3-21G//3-21 level of theory [41], which could then form the $CH_2{=}C{=}O^+$ ion by rupture of the $N\cdots CH_2$ weak bond in the complex. A more recent experimental and theoretical study [40] proposes that the acetamide cation (I) undergoes 1,3–H transfer to give not only tautomer II, the enol ion, but also tautomer III, an intermediate distonic cation $CH_2CONH_3^+$. The latter then dissociates to $CH_2{=}C{=}O^+ + NH_3$ by cleavage of the N–C bond. The dissociation energy, 1.54 eV, is smaller than the calculated I–III transition state energy, 1.89 eV [40], but a similar difference between experimental dissociation energies and calculated transition state energies has also been found for other acetamide cation dissociation reactions, as discussed later.

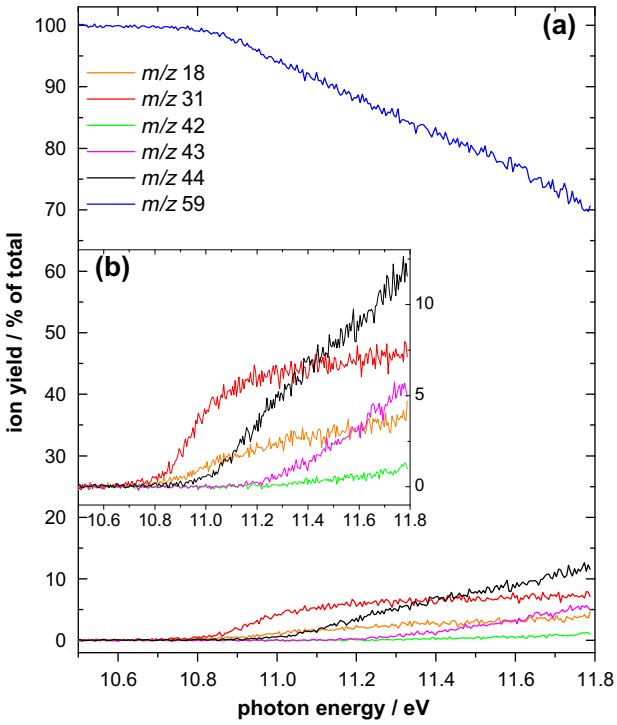

Fig. 7. Breakdown diagram of the parent ion and ionic fragments of acetamide between 10.5 and 11.8 eV. (a) Including the parent ion *m/z* = 59. (b) Zoom on fragment ions.

Morton [50] has shown, in a high resolution 70 eV EI study of the mass spectrum of acetamide, that the *m/z* 42 ion is due not only to the $CH_2{=}C{=}O^+$ ion but also to an ion of elemental composition $C_2H_4N^+$ formed in an OH-loss dissociation process, involving prior tautomerisation of the acetamide ion to $CH_3CO(H){=}NH^+$ (tautomer IV). The structure of the $C_2H_4N^+$ fragment ion was not determined and we note that there are 12 conceivable isomers having this composition [46]. The high resolution study found that the intensity of the $C_2H_4N^+$ ion is only about 7% of that of the $CH_2{=}C{=}O^+$ ion. At our mass resolution, a study of deuterated acetamide would be necessary to detect separately the deuterated versions of the two product ions of *m/z* 42 in hydrogenated acetamide. A calculation of the appearance energy of the OH-loss channel, based on experimental and theoretical thermochemical data for the 12 possible isomers of the $C_2H_4N^+$ ion [46] gives the range AE ($C_2H_4N^+$) = 11.42–15.1 eV. Our experimental AE = (11.20 ± 0.05) eV for *m/z* 42 is smaller than the lowest estimated value showing that at threshold this fragment ion is the ketene cation and not $C_2H_4N^+$. The observation that the relative intensity of ion *m/z* 42 is 1.6 times greater in the photon than in the 70 eV EI-MS (the latter is expected to mimic 35 eV photon excitation behaviour [53]) suggests

that the two products, $CH_2{=}C{=}O^+$ and $C_2H_4N^+$ do not have parallel ion yield curves as a function of energy.

4.3.4. m/z 41

The *m/z* 41 fragment ion is seen as a very weak signal in both photon impact and electron impact mass spectra. In our work it is first seen in a mass spectrum at 15.5 eV (not shown). However, even at higher photon energies, its intensity does hardly exceed the background noise level as can be seen in Figs. 2a–c. Two possible assignments of the dissociation channel are: (i) $C_2H_3N^+$ (+H_2O) and (ii) $HCCO^+$ (+NH_3 + H). These two channels have been found to have, respectively, ≈(2.8 ± 0.4)% and, ≈(8.6 ± 1.0)% of the intensity of the *m/z* 44 ion in a high resolution 70 eV EI mass spectrum [50], the total relative intensity for the *m/z* 41 ions being thus (11.4 ± 1.4)%. Other 70 eV EI mass spectral values are 7% [37] and 21% [38]. In our photon impact mass spectrum at 21 eV photon excitation energy the *m/z* 41 peak was 8.6 ± 1.0% of the *m/z* 44 peak, which is of a similar order to the sum of the resolved *m/z* 41 relative intensities in the high resolution 70 eV EI mass spectrum [50] and to the *m/z* 41 ion relative intensity in the NIST EI-MS [37]. Presumably the relative proportion of the $C_2H_3N^+$ and $HCCO^+$ ions is similar in the EI and photon impact cases. AEs calculated from thermodynamic data are 12.92 eV for $C_2H_3N^+$ and 15.95 eV for $HCCO^+$. Our observations are therefore consistent with the higher relative proportion of $HCCO^+$ to $C_2H_3N^+$ observed in the 70 eV EI mass spectra of Morton [50].

4.3.5. m/z 31

The two assignable ions of *m/z* 31 are $CH_3NH_2^+$ and its distonic isomer, $CH_2NH_3^+$. In both cases the neutral product is CO. The appearance energy of *m/z* 31 is AE = (10.71 ± 0.03) eV (Fig. 5a), in good agreement with a previous PIMS value AE = 10.77 ± 0.05 eV [14]. From our AE and $\Delta_fH(CO) = -1.145$ eV [37] we obtain as upper limiting values $\Delta_fH(CH_3NH_2^+/CH_2NH_3^+) = (9.386 \pm 0.038)$eV. The Lias et al. compilation [44] gives values $\Delta_fH(CH_3NH_2^+) = 8.725$ eV and $\Delta_fH(CH_2NH_3^+) \leq 8.715$ eV. The difference of the order of 670 meV with our experimental value could signal the existence of a large barrier in the formation of the *m/z* 31 ion by decarbonylation. Drewello et al. [41] have concluded from an experimental and theoretical study that, on electron impact, decarbonylation of the acetamide ion leads to formation of the distonic ion $CH_2NH_3^+$ with only an insignificant production of $CH_3NH_2^+$. The dissociation process involves isomerisation of the parent ion via intermediates that undergo hydrogen exchange between the CH_3CO and NH_2 groups, as discussed in a previous section. In a reaction scheme proposed by Mourges et al. [40] the process involves I → III isomerisation followed by further isomerisation of $CH_2CONH_3^+$ to the intermediate structure $NH_3CH_2CO^+$, which then dissociates to $CH_2NH_3^+ + CO$. This complex pathway could account for a high energy barrier in the decarbonylation reaction.

4.3.6. m/z 18

The ion signal at *m/z* 18 is assigned to NH_4^+, with HCCO as neutral product. The appearance energy AE = (10.77 ± 0.03) eV (Fig. 5b), in excellent agreement with the PIMS value AE = (10.77 ± 0.05) eV [14], is much below the H_2O ionization energy (12.62 eV [37]), which shows that the *m/z* 18 signal at 10.77 eV is not due to a water impurity, although a water impurity does exist and is seen at higher excitation energies.

The formation of NH_4^+ is suggested to involve prior isomerisation of tautomer I → III [40]. H-transfer must then occur before dissociation to $NH_4^+ + HCCO$. We remark that our measured dissociation energy, i.e. the difference between the AE and the parent's IE_{ad}, is (1.090 ± 0.045) eV (Table 1). This is 58% of the calculated I → III transition state energy, 1.89 eV [40]. The calculated I → II transition state energy, 1.16 eV [40] is also much greater than the experimental value (0.74 ± 0.06) eV from Ref. [14]. The ratio of the experimental to calculated energy value of the I → II transition is thus 64%, which is similar to the I → III transition state energy ratio. Therefore, if the theory overestimates the I → III transition energy, it could still be possible to produce NH_4 after tautomerisation.

From our appearance energy for *m/z* 18 and $\Delta_fH(HCCO) = (-1.838 \pm 0.091)$ eV [44], we obtain $\Delta_fH(NH_4^+) = (6.463 \pm 0.038)$eV. This represents a new limiting value for NH_4^+ since in the Lias et al. compilation [44] the value given is $\Delta_fH(NHn_4^+) = 6.528$eV, based on the proton affinity (8.85 eV) of NH_3.

We now examine whether, in our experiment, it would have been possible to detect the acetamide dissociation channel giving rise to $H_2O^+ + C_2H_3N$. From thermochemical data [37,44] we estimate the thermochemical threshold energy as 13.340 eV for $H_2O^+ + C_2H_3N$, assuming acetonitrile CH_3CN as neutral product. This value is within the water impurity ion yield spectrum region and so we are unable to affirm that this acetamide dissociation channel is active. The hygroscopic nature of acetamide is the most probable reason for the presence of the water impurity.

4.3.7. m/z 17

The appearance energy of the *m/z* 17 ion has been measured to be AE = (10.16 ± 0.03) eV (not shown). This is equal to the ionization energy of ammonia [37], so that we attribute the *m/z* 17 mass peak to an ammonia impurity in our photon impact study, most probably resulting from thermal dissociation of acetamide inside the oven. The neutral reaction $CH_3C(O)NH_2 \rightarrow NH_3 + CH_2CO$ is endothermic by about 100 kJ/mol and thus is favoured at higher temperatures. Also, we do not expect the reaction $CH_3C(O)NH_2 \rightarrow NH_3^+ + CH_2CO$ to occur, since its charge switch reaction $CH_3C(O)NH_2 \rightarrow NH_3 + CH_2CO^+$ is actually observed (*m/z* 42; cf. Section 4.3.3). We estimate the appearance energy of NH_3^+ formed by dissociative ionization of acetamide to be 11.654 eV. It would probably involve an enol ion intermediate, as discussed in Section 4.3.3.

We note that in the EI-MS, the ketene ion CH_2CO^+ is more intense than the ammonia ion. In these studies there is little evidence for an ammonia impurity [37,38]. Since $IE(CH_2CO) = (9.61 \pm 0.02)$ eV [44] and $IE(NH_3) = (10.16 \pm 0.01)$ eV, favouring the ketene ion channel is also in accordance with Stevenson's rule for charge switch reactions [54].

4.3.8. m/z 15

The ion yield curve for the *m/z* 15 ion (Fig. 6) is given in terms of a normalized ion intensity (and not percentage yield) since water (IE = 12.62 eV) is present as an impurity due to the hygroscopic nature of acetamide. We consider two possible assignments for the *m/z* 15 fragment ion, whose appearance energy is determined to be AE = (14.60 ± 0.03) eV in our study (Fig. 6): NH^+ and CH_3^+. From our AE, the channel $NH^+ + CH_3CHO$ would lead to the heat of formation $\Delta_fH(NH^+) = (13.849 \pm 0.042)$ eV, using $\Delta_fH(CH_3CHO) = (-1.718 \pm 0.04)$ eV [44]. The literature value Δ_fH (NH^+) is much higher, 17.39 eV [44], which shows that the *m/z* 15 fragment ion is most probably not NH^+.

We consider now the alternative channel $CH_3^+ + H_2NCO$, where our AE provides a value $\Delta_fH(CH_3^+) = (11.91 \pm 0.17)$ eV, using $\Delta_fH(H_2NCO) = (0.22 \pm 0.13)$ eV [55]. The literature value $\Delta_fH(CH_3^+) = 11.342$ eV [56], relatively close to ours in this case, implies however, that there is a high energy barrier (568 ± 170 meV) in this reaction which is somewhat unexpected since the reaction presumably involves a simple N–C bond rupture. It should be mentioned that the value of $\Delta_fH(H_2NCO)$ is possibly uncertain [55] since there are eleven isomers of this neutral species [57].

The $CH_3^+ + H_2NCO$ dissociation channel can be considered as the charge switch reaction with respect to formation of *m/z* 44. Since in the EI mass spectra, and in the photon impact mass spectra at $E_{exc} \geqslant 18$ eV, the intensity ratio of ions *m/z* 44 to 15 is ≈3.6, Stevenson's rule [54] would lead us to expect IE(H_2NCO) to be smaller than IE(CH_3) = 9.84 ± 0.01 eV [48]. From the values $\Delta_fH(H_2NCO)$ = 0.22 ± 0.13 eV [55] and $\Delta_fH(H_2NCO^+)$ = 6.90 ± 0.04 eV, the resulting IE(H_2NCO) = 6.78 ± 0.17 eV, is in agreement with the prediction from Stevenson's rule.

4.3.9. m/z 14

A very weak peak at *m/z* 14 is observed at E_{exc} = 17 eV, in very low intensity, but increasing towards higher energies to reach about 5% of the intensity of the parent ion at E_{exc} = 21 eV and ≈15% at E_{exc} = 24 eV. It cannot be N^+ resulting from dissociation of an N_2 impurity since the appearance energy of N^+ in the dissociative ionization of N_2 is 24.3 eV [37]. A possible assignment is to the CH_2^+ ion: Assuming that the dissociative reaction leads to the formation of $CH_2^+ + H_2NCHO$ (formamide), the fragment ion appearance energy calculated on the basis of thermochemical data [39,44] is 14.90 eV, consistent with our observations.

4.4. General features of the ionization yield curves of acetamide

Fig. 7 presents the dissociative ionization breakdown diagram for photon excitation energies between 10.5 and 11.8 eV. The parent ion yield curve decreases uniformly from the onset of dissociative ionization at 10.71 eV (CO loss, Table 1) up to 11.8 eV. This uniform decrease is consistent which the fact that there are no sharp changes of gradient in the fragment ion yield curves in this energy range, and that there are no new electronic states of the parent ion between the $1^2A''$ state at ≈ 10.1 eV and the $2^2A''$ state which lies at ≈ 13 eV [24,29].

In discussing the dissociative ionization results, 4 tautomers of the *m/z* 59 $C_2H_5NO^+$ ion have been considered. Our experimental results, as discussed above, and the work of Drewello et al. [41] and Mourges et al. [40] indicate that the principal dissociation possibilities involving these tautomers are:

$CH_3CONH_2^+$(I keto) : *m/z* 44 (CH_3 loss); *m/z* 43 (NH_2 loss); *m/z* 15 (H_2NCO loss)

$CH_2CO(H)NH_2^+$(II enol) : *m/z* 43 (NH_2 loss); *m/z* 42 (NH_3 loss)

$CH_2CONH_3^+$(III) : *m/z* 42 (NH_3loss); *m/z* 31 (CO loss); *m/z* 18 (HCCO loss)

$CH_3CO(H)NH^+$(IV) : *m/z* 42 (OH loss)(see section4.3.3).

Mourges et al. [40] have published a potential energy diagram for unimolecular reactions of $C_2H_5NO^+$ isomers, based on calculations performed at the G2(MP2) level. In this work, as mentioned previously, isomer II is calculated to be 820 meV below I, and III 190 meV below I, whereas IV is 473 meV above I. We note that the NH_2 and NH_3 loss channels via II have AE's at about 11.2 eV, whereas CO loss via the higher lying isomer III has an AE = 10.71 eV (lowest dissociation onset). However, the calculated energy barriers [40,41] in the various dissociation processes are consistent with these experimental results.

The *m/z* 31 and *m/z* 18 ion yield curves appear to rise at a similar rate, which is consistent with them both being formed via structure III. However, at 11.8 eV they appear to be close to reaching a plateau, of the order of 7.5% of total yield, for *m/z* 31, and 4%, for *m/z* 18. This is consistent with our observations at higher excitation energies and also with the 70 eV electron impact mass spectrum which exhibits relative abundances of ≈ 4% and ≈1% respectively for these two ions. The rise of the *m/z* 44 and *m/z* 43 yield curves are nearly but not quite parallel, which possibly reflects the fact that there are two possible NH_2 loss processes, involving structures I and II respectively, as mentioned in section 4.3.2. Furthermore, and as remarked earlier, we note that the intensity ratio of the H_2NCO^+ (*m/z* 44) to the CH_3CO^+ (*m/z* 43) ion in the 70 eV EI mass spectra, of the order of 1.4 [37,38], is similar to the intensity ratio of these ions in our photon impact mass spectra at excitation energies $E_{exc} \geqslant 12$ eV. This indicates that the $H_2NCO^+ + CH_3$ reaction channel is favoured over a large excitation energy range.

5. Conclusion

A VUV electron/ion coincidence study of acetamide was carried out using monochromatised synchrotron radiation over the photon energy range 8–24 eV. Photoion yield curves were measured for the parent ion and six fragment ions. The latter involve processes of neutral loss of the molecules CO and NH_3 and of the CH_3, NH_2, HCCO radicals, as well as H_2NCO. The adiabatic ionization energy of acetamide was determined as I.E. ($1^2A'$) = (9.71 ± 0.02) eV, in good agreement with a recent PIMS measurement. This σ ground state of the ion is shown to lie about 400 meV below the first excited π state, $1^2A''$, whose adiabatic energy is thus ≈10.1 eV. Coupling between the $1^2A'$ and $1^2A''$ states is invoked in discussions of the possible existence of isolated electronic states in the ion, and of the mechanisms of dissociative ionization.

The fragment ions were identified and the pathways of their formation were proposed on the basis of their appearance energies, aided by thermochemical data and the published results of electron and photon impact mass spectral studies. Heats of formation are derived for all ions detected and are compared with literature values where they exist; the values determined are often new or revised with respect to previous publications.

Finally, we remark that H Ly-α emission (10.21 eV), which is important in the VUV in both the solar system and in the interstellar medium (ISM), is 500 meV above the ionization energy of acetamide. We can estimate that at the HI limit, 13.6 eV in the ISM, the total ionization yield of acetamide will be of the order of 56%, using a rule of thumb that is valid for many molecules [58]. The acetamide parent ion is stable up to 10.71 eV (CO-loss channel) i.e. well above the Ly-α emission but 2.89 eV below the HI limit at 13.6 eV; the total ionization yield is estimated to be of the order of 15% at 10.71 eV. Generally, the quantum yields of fragment cation formation from acetamide by VUV radiation are weak below 13.6 eV (cf. for example Fig. 7), so that in interstellar HI regions the parent ion would predominate.

These results should be integrated into models concerning the presence and possible survival of this prebiotic molecule in space. They particularly concern the possibility of observation of acetamide in the ISM and in comets, where this species would be subject to UV and VUV irradiation. However, we note that absorption and ionization cross sections are still needed for this molecule to compute survival rates in given radiation fields. Also, experimental data on neutral dissociation would be useful for astrophysical applications.

Acknowledgements

We acknowledge support from the CNRS GDR "Exobiologie" and the CNRS interdisciplinary programme *"Environnement planétaire et origine de la vie"* (PID EPOV; programme "PhotoBio"). We are indebted to Jean-François Gil for his technical help on the SAPHIRS experiment and on the DESIRS beamline. We also thank the general staff of Soleil for running the facility.

References

[1] R. Saladino, C. Crestini, G. Costanzo, R. Negri, E. Di Mauro, Bioorg. Med. Chem. 9 (2001) 1249;
G. Costanzo, R. Saladino, C. Crestini, F. Ciciriello, E. Di Mauro, BMC Evol. Biol. 7 (Suppl. 2) (2007) S1.

[2] (a) Formic Acid: S. Leach, M. Schwell, F. Dulieu, J.L. Chotin, H.-W. Jochims, H. Baumgärtel, Phys. Chem. Chem. Phys. 4 (2002) 5025;
M. Schwell, F. Dulieu, H.-W. Jochims, J.-H. Fillion, J.-L. Lemaire, H. Baumgärtel, S. Leach, J. Phys. Chem. A 106 (2002) 10908;
(b) Ammonia: S. Leach, H.-W. Jochims, H. Baumgärtel, Phys. Chem. Chem. Phys. 7 (2005) 900;
(c) Acetic acid: S. Leach, M. Schwell, S. Un, H.-W. Jochims, H. Baumgärtel, Chem. Phys. 321 (2006) 159;
S. Leach, M. Schwell, H.-W. Jochims, H. Baumgärtel, Chem. Phys. 321 (2006) 171;
(d) Acetonitrile: S. Leach, M. Schwell, S. Un, H.-W. Jochims, H. Baumgärtel, Chem. Phys. 344 (2008) 147;
M. Schwell, H.-W. Jochims, H. Baumgärtel, S. Leach, Chem. Phys. 344 (2008) 164.

[3] H.-W. Jochims, M. Schwell, J.L. Chotin, M. Clemino, F. Dulieu, H. Baumgärtel, S. Leach, Chem. Phys. 298 (2004) 279.

[4] M. Schwell, H.-W. Jochims, H. Baumgärtel, S. Leach, Chem. Phys. 353 (2008) 145.

[5] H.-W. Jochims, M. Schwell, H. Baumgärtel, S. Leach, Chem. Phys. 314 (2005) 263.

[6] S. Pilling, A.F. Lago, L.H. Coutinho, R.B. de Castilho, G.G.B. de Souza, A.N. de Brito, Rapid Commun. Mass Spectrom. 21 (2007) 3646;
O. Plekan, V. Feyer, R. Richter, M. Coreno, M. De Simone, K.C. Prince, Chem. Phys. 334 (2007) 53;
P. Ehrenfreund, M.P. Bernstein, J.P. Dworkin, S.A. Sandford, J. Allamandola, Astrophys. J. 550 (2001) L95.

[7] I. Ribias, E.F. Guinan, M. Güdel, M. Audard, Astrophys. J. 622 (2005) 680;
M. Gargaud, B. Barbier, H. Martin, J. Reisse (Eds.), Lectures in Astrobiology, Springer, Berlin, 2005;
C. Chyba, C. Sagan, Nature 355 (1992) 125.

[8] S. Miller, in: A. Brack (Ed.), The Molecular Origin of Life, Cambridge Univ. Press, Cambridge, UK, 1998, p. 59.

[9] J.-L. Lemaire, F. Combes (Eds.), Molecules in Space and in the Laboratory, Observatoire de Paris, 2007.

[10] R.T. Garrod, S.L. Widicus Weaver, E. Herbst, Astrophys. J. 682 (2008) 283.

[11] J.M. Hollis, F.J. Lovas, A.J. Remijan, P.R. Jewell, V.V. Ilyushin, I. Kleiner, Astrophys. J. 643 (2006) L25.

[12] L. Allamandola, M.P. Bernstein, S.A. Sandford, R.L. Walker, Space Sci. Rev. 90 (1999) 219.

[13] K. Watanabe, T. Nakayama, J. Mottl, J. Quant. Spectrosc. Radiat. Transfer 2 (1962) 369.

[14] D. Schröder, J. Loos, R. Thissen, O. Dutuit, P. Mourges, H.-E. Audier, C. Lifshitz, H. Schwarz, Angew. Chem. Int. Ed. 41 (2002) 2748.

[15] G. Fogarasi, P. Pulay, F. Török, J.E. Boggs, J. Molec. Struct. 57 (1979) 259.

[16] L. Serrano-Andrés, M.P. Fülscher, J. Am. Chem. Soc. 118 (1996) 12190.

[17] M. Kitano, K. Kuchitsu, Bull. Chem. Soc. Jpn. 46 (1973) 3048.

[18] G.A. Jeffrey, J.R. Ruble, R.K. McMullan, D.J. DeFrees, J.S. Binkley, J.A. Pople, Acta Cryst. B36 (1980) 2292.

[19] E.L. Hansen, N.W. Larsen, M. Nicolaisen, Chem. Phys. Lett. 69 (1980) 327.

[20] R.A. Kydd, A.R.C. Dunham, J. Molec. Struct. 69 (1980) 79.

[21] L. Radom, N.V. Riggs, Aust. J. Chem. 35 (1982) 1071.

[22] T. Drakenberg, Tetrahedron Lett. 13 (1972) 1743.

[23] P.J. Jasien, W.J. Stevens, M. Krauss, J. Molec. Struct. Theochem 139 (1986) 197.

[24] L. Asbrink, A. Svensson, W. von Niessen, G. Bieri, J. Electron Spectrosc. Relat. Phenom. 24 (1981) 293.

[25] G.W. Mines, H.W. Thompson, Spectrochim. Acta 31A (1975) 137.

[26] D.A. Sweigart, D.W. Turner, J. Am. Chem. Soc. 94 (1972) 5592.

[27] N. Kishimoto, Y. Osada, K. Ohno, J. Electron Spectrosc. Relat. Phenom. 114–116 (2001) 183.

[28] S.P. McGlynn, J.L. Meeks, J. Electron Spectrosc. Relat. Phenom. 6 (1975) 269.

[29] J.L. Meeks, J.F. Arnett, D. Larson, S.P. McGlynn, Chem. Phys. Lett. 30 (1975) 190.

[30] <http://www.synchrotron-soleil.fr/Recherche/LignesLumiere/DESIRS>.

[31] L. Nahon, C. Alcaraz, J.L. Marlats, B. Lagarde, F. Polack, R. Thissen, D. Lepère, K. Ito, Rev. Sci. Inst. 72 (2001) 1320.

[32] B. Mercier, M. Compin, C. Prevost, G. Bellec, R. Thissen, O. Dutuit, L. Nahon, J. Vac. Sci. Technol. A 18 (2000) 2533.

[33] G.A. Garcia, H. Soldi-Lose, L. Nahon, Rev. Sci. Instr. 80 (2009) 023102.

[34] F. Gaie-Levrel, C. Gutlé, H.W. Jochims, E. Rühl, M. Schwell, J. Phys. Chem. A 112 (2008) 5138.

[35] W.A. Chupka, J. Chem. Phys. 30 (1959) 191.

[36] J. Oberheide, P. Wilhelms, M. Zimmer, Meas. Sci. Technol. 8 (1997) 351.

[37] NIST Chemistry Webbook, National Institute of Standards and Technology Reference Database, June 2005. <http://webbook.nist.gov>.

[38] J.A. Gilpin, Anal. Chem. 31 (1959) 935.

[39] S. Leach, H.-W. Jochims, H. Baumgärtel, J. Phys. Chem. A 114 (2010) 4847.

[40] P. Mourges, J. Chamot-Rooke, H. Nedev, H.-E. Audier, J. Mass Spectrom. 36 (2001) 102.

[41] T. Drewello, N. Heinrich, W.P.M. Maas, N.M.M. Nibbering, T. Weiske, H. Schwartz, J. Am. Chem. Soc. 109 (1987) 4810.

[42] H.M. Rosenstock, Adv. Mass Spectrom. 4 (1968) 523.

[43] S. Leach, G. Dujardin, G. Taieb, J. Chim. Phys. 77 (1980) 705.

[44] S.G. Lias, J.E. Bartmess, J.F. Liebman, J.L. Holmes, R.D. Levin, W.G. Mallard, J. Phys. Chem. Ref. Data 17 (Suppl. 1) (1988).

[45] F.I. Vilesov, Dokl. Phys. Chem. 132 (1960) 521.

[46] J.L. Holmes, C. Aubry, P.M. Mayer, Assigning Structures to Ions in Mass Spectrometry, CRC Press, Boca Raton, 2007.

[47] C.E.C.A. Hop, J.L. Holmes, P.A. Ruttink, G. Schaftenaar, J.K. Terlouw, Chem. Phys. Lett. 156 (1989) 251.

[48] A.G. Loudon, K.S. Webb, Org. Mass Spectrom. 12 (1977) 283.

[49] R.H. Nobes, W.J. Bouma, L. Radom, J. Am. Chem. Soc. 105 (1983) 309.

[50] T.H. Morton, Org. Mass Spectrom. 26 (1991) 18.

[51] C. Aubry, J.L. Holmes, J.K. Terlouw, J. Phys. Chem. A 101 (1997) 5958;
J.C. Traeger, Int. J. Mass Spectrom. 194 (2000) 261.

[52] R.L. Nuttall, A.H. Laufer, M.V. Kilday, J. Chem. Thermodyn. 3 (1971) 167.

[53] S. Leach, J.H.D. Eland, S.D. Price, J. Phys. Chem. 93 (1989) 7575.

[54] D.P. Stevenson, Disc. Faraday Soc. 10 (1951) 35.

[55] S. Leach, N. Champion, H.-W. Jochims, H. Baumgärtel, Chem. Phys. 376 (2010) 10.

[56] J.C. Traeger, B.M. Kompe, in: J.A. Martinho Simoes, A. Greenberg, J.F. Liebman (Eds.), Energetics of Organic Free Radicals, Blackie Academic and Professional, London, 1996, p. 59.

[57] W.A. Shapley, G.B. Backsay, J. Phys. Chem. 103 (1999) 4505.

[58] H.-W. Jochims, H. Baumgärtel, S. Leach, Astron. Astrophys. 314 (1996) 1003.